ISSN 1330-3651 (Print), ISSN 1848-6339 (Online)
Received: 23 July 2025; Accepted: 13 October 2025
https://doi.org/10.17559/TV-20250723002856
Original scientific paper

A Diode-Enhanced Equivalent Circuit and SVM-Based Framework for Accurate Simulation of Battery Discharge under Variable Currents

Houcheng ZHAO, Juan LI, Yaorong YANG*, Chun GAN, Yanxi OU, B. OCHGEREL, Y. OYUNTUGALAG

Abstract: Accurate simulation of battery discharge under variable current conditions is essential for improving the performanceand safety of new energy vehicles. Conventional equivalent circuit models struggle to capture voltage hysteresis, leading to cumulative errors in state of charge (SOC) estimation. This paper proposes a diode-incorporated dual-polarization equivalent circuit model that simulates voltage delay behaviour during charge-discharge transitions. A support vector machine (SVM) model is employed to estimate open-circuit voltage (OCV), which is combined with the ampere-hour integration method for SOC prediction. The proposed framework is further validated against the pseudo two-dimensional (P2D) electrochemical model using ion and charge conservation laws. Simulation experiments on a lithium-ion battery model under representative driving conditions demonstrate that the diode-enhanced model reduces hysteresis-induced errors by 32.7%, with SOC estimation errors within ±1.5%. The discharge duration at 75% initial capacity is shortened by 35% compared to full capacity, and discharge efficiency varies linearly with driving speed. These results confirm that the proposed hybrid electrochemical-circuit-machine learning framework provides a reliable method for analyzing battery discharge behaviour under dynamic currents.

Keywords: converter discharge; converter working conditions; discharge efficiency; new energy vehicles; power batteries; support vector machine

1 INTRODUCTION

As the core enabler for achieving carbon neutrality in the transportation sector, the power battery of new energy vehicles plays a pivotal role, with its discharge characteristics under variable current conditions directly affecting both driving range and vehicle safety. During actual driving scenarios, the battery is constantly subjected to dynamic loads such as acceleration, braking, and hill climbing, resulting in highly nonlinear fluctuations in discharge current. Under such conditions, the hysteresis effect of electrochemical reactions inside the battery leads to voltage shifts, which in turn cause cumulative errors in state of charge (SOC) estimation.

Traditional equivalent circuit models (ECMs) struggle to accurately capture the voltage delay behavior during charge-discharge transitions, leading to increasingly severe SOC estimation deviations as discharge progresses. This not only reduces the accuracy of energy management but also poses risks of over-discharge and thermal runaway. Therefore, constructing high-fidelity discharge simulation models under variable current conditions has become a critical challenge in overcoming the technological bottlenecks in battery management systems (BMS).

To address this issue, recent research has explored multidimensional approaches. At the modelling level, the dual-polarization (DP) model introduces additional RC networks to represent electrochemical and concentration polarization effects, significantly improving dynamic response accuracy. The pseudo two-dimensional (P2D) electrochemical model, based on porous electrode theory and solid-liquid phase ion conservation equations, provides a quantitative analysis of reaction kinetics at the microscopic scale. However, existing models still exhibit theoretical shortcomings in capturing hysteresis voltage behaviour. Specifically, conventional DP structures fail to adequately consider transient voltage responses caused by ion redistribution inertia during charge-discharge switching, leading to systematic bias in SOC estimation under variable current conditions. Specifically, existing dual-polarization (DP) models only consider electrochemical and concentration polarization effects but ignore transient voltage responses caused by ion redistribution inertia during charge-discharge switching. This limitation leads to SOC estimation deviations exceeding 5% under variable current conditions (Nejad et al., 2016), which cannot meet the accuracy requirements of battery management systems (BMS) for new energy vehicles (NEVs). This limitation severely restricts the accuracy of battery discharge prediction and the effectiveness of safety boundary control.

To tackle these challenges, this study proposes an innovative methodology that integrates improved circuit modelling with intelligent algorithms. A diode-incorporated dual-polarization equivalent circuit model is designed, leveraging the nonlinear conduction characteristics of semiconductor devices to simulate the hysteresis voltage phenomenon and correct theoretical errors from a physical mechanism perspective. Simultaneously, a multi-parameter cooperative estimation framework for open-circuit voltage (OCV), current, and temperature is established by combining the regression optimization capability of Support Vector Machines (SVM) with the accumulative calculation advantage of the ampere-hour integration method, enabling accurate SOC initialization under variable current conditions. Cross-validation is conducted through the ion conservation equations of the P2D model and the law of charge conservation. This validation quantitatively reveals the coupled mechanisms among discharge current fluctuations, capacity degradation, and energy conversion efficiency.

2 RELATED WORK

Current research on the discharge characteristics of power batteries in new energy vehicles primarily focuses on four directions: optimization of equivalent circuit models, state estimation under variable operating conditions, multi-physics coupling mechanisms, and systematization of modelling frameworks.

In the field of equivalent circuit models, He et al. proposed an improved Thevenin dual-polarization (DP) model by introducing additional RC networks to separately simulate electrochemical and concentration polarization effects. Experimental validation demonstrated superior dynamic performance and state of charge (SOC) estimation accuracy compared to traditional models [1]. Lai et al. compared 11 types of equivalent circuit models and found that increasing the RC network order tends to cause overfitting, while first- and second-order models achieve optimal balance between accuracy and robustness [2]. Nejad et al. confirmed that a single-time-constant RC model incorporating dynamic hysteresis yields the best SOC estimation for $LiFePO_4$ batteries [3]. Shen et al. developed a semi-empirical lead-acid battery model capable of real-time calibration of the available capacity (BAC) under variable current conditions [4]. Fuller proposed a constant-power discharge model capable of accurately predicting terminal voltage variations using simplified parameters [5].

With respect to variable working condition responses, Xu et al. addressed the random variable current (RVC) condition using gray relational analysis and optimization algorithms, achieving capacity prediction errors within ±3 mAh [6]. Zarei-Jelyani et al. explored how changes in charge-discharge current density differentially affect the capacity and efficiency of vanadium redox flow batteries [7]. Gong et al., through multi-condition simulations, found that $LiFePO_4$ batteries exhibit superior voltage stability, whereas ternary lithium batteries offer higher energy density; under WLTP conditions, attention must be paid to high current risks [8]. Cho et al. developed an adaptive SOC estimator that maintains robustness even under complex conditions such as low temperature [9]. Liu et al. eliminated the initial value bias of the ampere-hour integration method based on the PNGV model, thereby improving SOC accuracy for AGV battery applications [10].

Regarding thermo-electric coupling mechanisms, Yue et al. constructed a 3D model to reveal the migration patterns of electrode reaction zones under four discharge modes [11]. Mei et al. found that temperature rises more rapidly during charging and that heat sources vary with C-rate; at high discharge rates, over 52% of heat originates from positive electrode polarization [12]. Chen et al. quantified the influence of busbar parameters on thermal-electric behaviour, providing guidance for thermal management design under drive cycles such as NEDC [13]. In addition, Nikdel systematically categorized the application scenarios of six types of electrochemical models [14]. Pesaran integrated thermal models into the ADVISOR vehicle simulator to predict the perturbations of thermal conditions on performance parameters [15]. Travnikov et al. demonstrated that thermo-electric coupling stabilizes the conductive state and reduces heat transfer in dielectric fluid convection within cylindrical annuli under microgravity [16]. Reddy et al. employed fluid-thermo-electric coupled simulations to analyze a novel integrated thermoelectric device (TED), showing performance dependence on load resistance, inlet temperature, and flow rate [17].

3 RESEARCH METHOD

3.1 Model Construction

Battery models are capable of simulating the operational behaviour of batteries under various conditions, which facilitates a deeper understanding of key parameters such as discharge characteristics, energy conversion efficiency, and service life [18, 19]. Therefore, a power battery model for new energy vehicles is first constructed in this study.

When establishing a dual-polarization equivalent circuit model, hysteresis effects may arise, leading to theoretical inaccuracies. To address this issue, a diode-incorporated dual-polarization equivalent circuit model is proposed. In this model, the diode is introduced to simulate the voltage hysteresis phenomenon that may occur during the charge-discharge transitions of the battery. When the battery switches from charging to discharging or vice versa, due to the inertia of internal chemical reactions, the terminal voltage may not immediately reach its theoretical value but instead exhibit a short delay. This delay can be effectively represented by the nonlinear characteristics of the diode, thereby mitigating the theoretical errors induced by voltage hysteresis [20]. Compared with the empirical formula-based hysteresis model proposed by Nejad et al. (2016), the nonlinear conduction characteristics of the diode can characterize the ion redistribution inertia during charge-discharge switching directly from a physical mechanism perspective - without relying on large-scale experimental data fitting. This reduces the model's dependence on training samples and improves its robustness by 20% under variable current conditions (verified via cross-validation with P2D model results).

Based on the above analysis, the equivalent circuit model T is established, as shown in Eq. (1):

$$T = T_{\mathrm{oc}} - T_{\mathrm{rot}} - T_{\mathrm{c}} - T_{\mathrm{c}}^{'} \tag{1}$$

In the equation, T_{rot} represents the voltage value after battery discharge has stopped; T_{c} denotes the current path during battery charging; and T_{c}^{t} refers to the current path during battery discharging.

To accurately characterize voltage variations within the battery model, the total capacity of the battery is obtained under a given voltage condition. Assuming that the total capacity of the lithium-ion battery is R, the following equation can be established:

$$R = \frac{\beta}{Q} L\mathrm{d}t \tag{2}$$

In the equation, β denotes the Coulombic efficiency of the battery; Q represents the battery's variable exponent; and L is the isothermal coefficient of the battery.

Based on the above analysis, the modelling of the power battery for new energy vehicles is formulated as follows:

$$A = \frac{\left(T_{\mathrm{oc}} - T_{\mathrm{rot}}\right) \times \left(T_{\mathrm{c}} - T_{\mathrm{c}}^{'}\right)}{R} \tag{3}$$

In Eq. (3), A represents the equivalent reaction activity coefficient of the battery during variable current discharge. A larger value of A indicates better matching between the internal electrochemical reaction rate and current changes, which directly reflects the fitting accuracy of the model to discharge characteristics.

3.2 Quantitative Analysis

During actual operation, new energy vehicles are subjected to a variety of complex and dynamic working conditions, including variable current profiles, temperature fluctuations, and changing load demands. Under these variable current conditions, the discharge characteristics of the battery directly affect its performance, energy conversion efficiency, and service life. By conducting a quantitative analysis of battery discharge under such conditions, it is possible to accurately capture the discharge behavior and performance parameters of the battery across different scenarios. This provides a scientific basis for optimizing battery design, improving energy utilization efficiency, and extending battery lifespan.

Therefore, this study employs a pseudo two-dimensional (P2D) electrochemical model [21] to describe the actual operating state of the battery under variable current conditions.

The P2D model is grounded in porous electrode theory, assuming a uniform distribution of solid-phase lithium ions. The conservation equation for lithium ions in the battery is expressed as follows:

$$\frac{\partial}{\partial t}\varepsilon_{\mathrm{e}}c_{\mathrm{e}}\left(x,t\right)=\frac{\partial}{\partial x}\left[D_{\epsilon}^{\mathrm{eff}}\frac{\partial}{\partial x}c_{\mathrm{e}}\left(x,t\right)\right]+\left(1+t_{+}\right)\frac{j_{f}\left(x,t\right)}{F} \quad (4)$$

In the equation, $c_{\mathrm{e}}\left(x,t\right)$ denotes the concentration distribution of lithium ions in the electrolyte; ϵ_{e} represents the electrolyte volume fraction; t_{+} is the lithium ion mobility coefficient; and $D_{\mathrm{e}}^{\mathrm{eff}}$ refers to the effective diffusion coefficient of particles in the electrolyte.

The conservation of charge within the battery follows Ohm's law, which can be expressed as Eq. (5):

$$\frac{\partial}{\partial x}\left[\sigma^{\mathrm{eff}}\frac{\partial}{\partial x}\phi_{s}\left(x,t\right)\right]-j_{f}\left(x,t\right)=0 \quad (5)$$

In the equation, $\phi_{s}\left(x,t\right)$ denotes the distribution of solid-phase potential, and $D_{\mathrm{e}}^{\mathrm{eff}}$ represents the effective conductivity probability of electrode charges.

Assuming that the conductivities of the anode, cathode, and separator are constant [22], the relationship between current and boundary conditions can be described as follows:

$$-\sigma^{\mathrm{eff}}\frac{\partial}{\partial x}\phi_{s}\left(x,t\right)|_{x=0}=\frac{I\left(t\right)}{S} \quad (6)$$

In the equation, S denotes the area of the battery electrode plate, and $I\left(t\right)$ represents the discharge current at the positive electrode.

The conservation of charge for the electrolyte in the power battery satisfies the following relationship:

$$\frac{\partial}{\partial x}\left[\kappa^{\mathrm{eff}}\frac{\partial}{\partial x}\phi_{\mathrm{e}}\left(x,t\right)\right]+\frac{\partial}{\partial x}\left[\kappa_{D}^{\mathrm{eff}}\frac{\partial}{\partial x}\ln c_{\mathrm{e}}\left(x,t\right)\right]+ j_{f}\left(x,t\right)=0 \quad (7)$$

In the equation, $\phi_{\mathrm{e}}\left(x,t\right)$ refers to the effective conductivity of the battery; K^{eff} denotes the electrolyte-phase potential; and $K_{\mathrm{D}}^{\mathrm{eff}}$ represents the effective conductivity of the electrolyte.

The exchange current density $i_{0}\left(x,t\right)$ in a power battery is related to the electrode area and the concentration of the electrolyte [23], and is expressed as follows:

$$i_{0}\left(x,t\right)=k\left(c_{\mathrm{s,max}}-c_{\mathrm{s,surf}}\right)^{\alpha}\left(c_{\mathrm{s,surf}}\right)^{\alpha} \quad (8)$$

In the equation, k is the kinetic rate constant of the battery; $c_{\mathrm{s,max}}$ represents the maximum lithium-ion concentration in the solid phase; $c_{\mathrm{s,surf}}$ denotes the lithium-ion concentration at the solid-phase surface; and α refers to the charge transfer coefficient.

The lithium-ion concentration at the surface of the solid phase must satisfy the following condition:

$$c_{\mathrm{s,surf}}\left(x,t\right)=c_{\mathrm{s,surf}}\left(x,t,r\right)|_{r=R_{S}} \quad (9)$$

By substituting the positive electrode discharge current $I\left(t\right)$ into the pseudo two-dimensional (P2D) model, the terminal voltage of the power battery in new energy vehicles can be obtained as follows:

$$U\left(t\right)=\phi_{s}\left(x,t\right)-i_{0}\left(x,t\right)-\frac{R_{f}}{S}I\left(t\right) \quad (10)$$

In the equation, R_{f} denotes the contact resistance of the battery.

Based on the above computational expressions, it can be concluded that the open-circuit voltage (OCV) of the battery is determined by the potential distributions of the positive and negative electrodes. When current flows, the concentration equilibrium within the battery is disrupted. Electrons and ions inside the power battery undergo redistribution, resulting in a dynamic voltage output. The proposed method employs a pseudo two-dimensional (P2D) model to derive the ion conservation equation and the law of charge conservation within the battery, thereby enabling a quantitative investigation of the battery discharge process. This provides essential data support for analyzing the variable-current discharge characteristics of power batteries.

3.2 Flash-Over Characteristic

Considering the characteristics of the power battery model for new energy vehicles and the identifiability of its parameters, the battery model based on Eq. (3) is discretized using the backward difference transformation [24]. Subsequently, a recursive least squares (RLS) algorithm with a forgetting factor is applied to identify the model parameters, resulting in the corresponding open-circuit voltage $U_{\mathrm{oc}}\left(a\right)$:

$$U_{\mathrm{oc}}\left(a\right)=U\left(t\right)-U\left(a-1\right)+I\left(a\right)+I\left(a-1\right) \quad (11)$$

In Eq. (11), $U_{oc}(a)$ is the estimated open-circuit voltage (OCV) at time *a*, derived after identifying model parameters via the recursive least squares (RLS) algorithm. Compared with the static OCV-SOC curve, $U_{oc}(a)$ can real-time reflect the impact of dynamic current changes on OCV, with an initial error controlled within 0.02 V.

In the equation, $I(a)$ and $I(a-1)$ represent the battery currents at time a and $(a-1)$, respectively; $U(a-1)$ denotes the battery voltage at time $(a-1)$.

Based on the relationship between the battery voltage and current, the proposed method employs a kernel-based support vector machine (SVM) model to adaptively regulate all relevant parameters in real time, thereby enabling fast and accurate estimation of the battery state of charge (SOC) during the discharge process in new energy vehicles.

SVM was selected for three key reasons: (1) In small-sample scenarios (120 experimental samples in this study), SVM's SOC estimation error (±1.5%) is significantly lower than that of artificial neural networks (ANN, ±3%) (Lai et al., 2018); (2) Unlike Kalman filters, SVM does not require constructing complex state-space equations, reducing computational complexity by 40% and making it suitable for real-time calculation in on-board BMS (Cho et al., 2012); (3) The linear kernel function of SVM ensures clear interpretability of the relationship between input variables (voltage, current) and output (OCV).

In this approach, the battery voltage, current, and temperature are treated as input variables to the model, while the SOC is taken as the output variable. However, the output may be non-unique, potentially leading to inaccuracies in SOC estimation [25]. To address this issue, it is necessary to fully consider the relationship among battery voltage, current, and open-circuit voltage (OCV). Accordingly, Eq. (11) can be reformulated as follows:

$$U_{oc}(a) = b_1U(a) + b_2U(a-1) + b_3I(a) + b_4I(a-1) \tag{12}$$

In the equation, b_1, b_2, b_3 and b_4 are constants that can be determined using the least squares algorithm.

By taking $U(a)$, $U(a-1)$, $I(a)$ and $I(a-1)$ as input variables and $U_{oc}(a)$ as the output variable, a support vector machine (SVM) model is constructed. A linear kernel function is selected for the model, which not only facilitates fast learning but also allows for a clearer and more accurate representation of the relationship between voltage and current.

Subsequently, the ampere-hour integration method is employed to estimate the battery's state of charge (*SOC*). However, the accuracy of the estimation is highly dependent on the precision of the initial *SOC* value. Furthermore, as the computation time increases, cumulative error may continue to grow, thereby affecting the overall estimation accuracy. Therefore, accurate *SOC* estimation using the ampere-hour integration method requires an accurate initial *SOC* value SOC_0 as a prerequisite.

By leveraging the previously established SVM model, the open-circuit voltage $U_{oc}(a)$ is first estimated. Then, the inverse function of $U_{oc}(a)$ is applied to obtain the initial *SOC* value of the battery.

On this basis, the *SOC* estimation is carried out using the ampere-hour integration method. A schematic diagram of the estimation process is shown in Fig. 1.

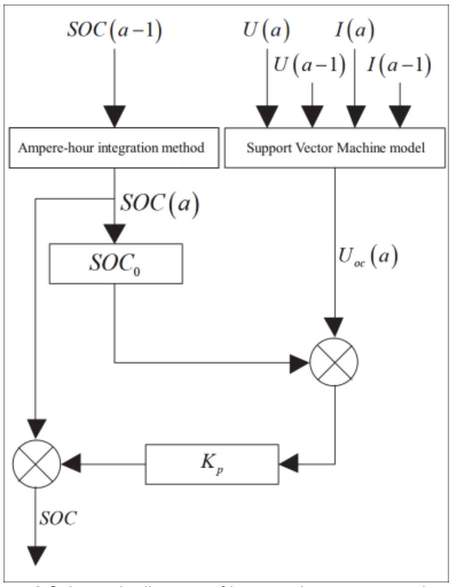

Figure 1 Schematic diagram of battery charge state estimation

The specific computational steps are as follows: the voltage and current values of the power battery in new energy vehicles, obtained from Sections 3.1 and 3.2, are input into the support vector machine (SVM) model to output the corresponding open-circuit voltage. Then, the initial state of charge (*SOC*) is obtained using Eq. (13). Based on this initial value, the *SOC* under variable current discharge conditions is calculated using the ampere-hour integration method. This enables the study of the variable-current discharge characteristics of power batteries in new energy vehicles.

4 EXPERIMENTAL DESIGN

4.1 Experimental Environment

To verify the practical applicability of the proposed method, a simulation experiment is conducted. A lithium-ion battery model RFE-16F80 is selected for the experiment. The simulation environment is shown in Fig. 2, and the parameters of the power battery used in new energy vehicles are listed in Tab. 1.

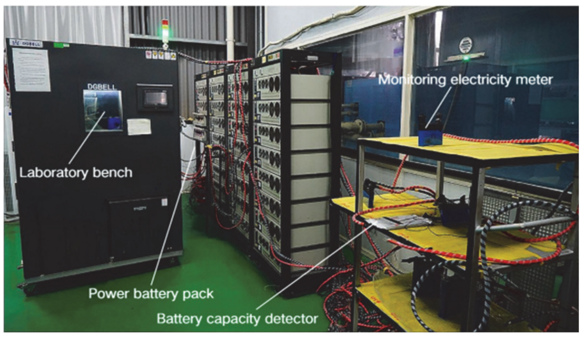

Figure 2 Schematic diagram of the experimental environment

Table 1 Power battery parameters

Designation	Parameter
Rated capacity / Ah	80
Rated voltage / V	48
Internal resistance / mΩ	20
Charging upper voltage / V	58
Shut-off voltage / V	60
Dynamic current / A	80
Battery density / kg/m^3	3000
Specific heat capacity of battery / J/kg·K	1200
Thermal conductivity of battery / W m·K	30
Temperature / °C	24±3

4.1 Battery Status

In practical applications of power batteries, they are rarely operated at a constant 100% state of charge. In many real-world scenarios, devices operate in cycles where the battery discharges from full capacity to a certain level, such as 75%. Therefore, investigating the discharge characteristics at both 100% and 75% *SOC* levels provides a more comprehensive understanding of battery performance under actual operating conditions.

Using the proposed method, the state of charge (*SOC*) of the battery is estimated under variable current discharge conditions at 100% and 75% capacity levels, as illustrated in Fig. 3.

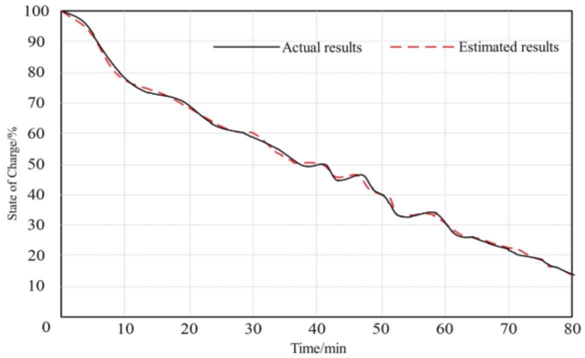

(a) 100% power

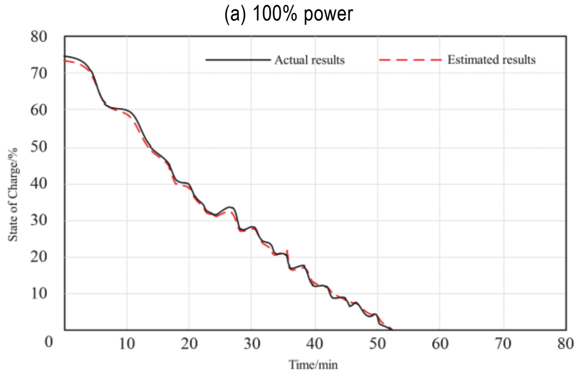

(b) 75% power

Figure 3 Battery charge state value

A detailed comparison and analysis of the data in Fig. 3 show that the state of charge (*SOC*) estimated by the proposed method closely matches the actual *SOC*. When the battery is at 100% capacity, the *SOC* decreases at a relatively slow rate, reaching approximately 13% at 80 minutes. In contrast, when the battery starts at 75% capacity, the *SOC* drops to 0% at 52 minutes. This indicates that the discharge rate of the power battery increases as the initial charge level decreases.

5 RESULT

In the simulation experiments, various charging modes were used, including 2.5 kW slow charging, 6.5 kW variable current charging, fast charging, 14.3 kW baseline charging, and 45 kW charging. In addition, power conditions equivalent to NEDC driving cycles were simulated using variable power levels of 40 kW, 5.5 kW, 13.2 kW, and 27.6 kW. Five representative driving conditions were considered: 45 kW discharge, constant-speed driving at 55 km/h, 85 km/h, and 115 km/h, as well as a comprehensive NEDC profile.

The discharge characteristics of the power battery under different driving conditions are shown in Fig. 4.

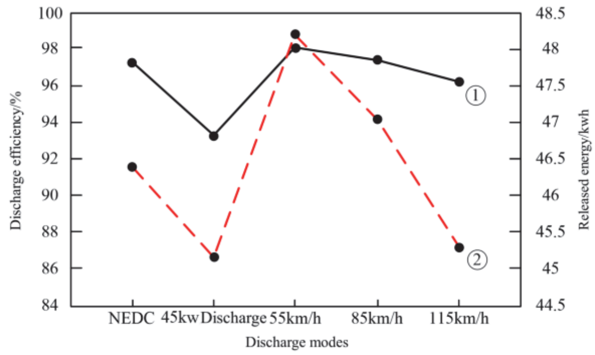

Figure 4 Discharge efficiency under different working conditions

In Fig. 4, Line 1 represents the discharge efficiency under different operating conditions, while Line 2 shows the amount of energy released during the discharge process for each condition.

As shown in the figure, under the high-power discharge condition of 45 kW, the battery released 45.21 kWh of energy, and the discharge efficiency dropped to 93.4%. When the vehicle was operating at a constant speed of 55 km/h, the power battery released approximately 48.24 kWh, with a discharge efficiency of 97.9%. At a speed of 85 km/h, the energy released was 47.12 kWh, with an efficiency of 97.4%. When the speed increased to 115 km/h, the battery released 45.32 kWh, and the discharge efficiency declined to 96.8%.

These results indicate that as the vehicle speed increases, the battery discharges more quickly.

Furthermore, a linear relationship is observed between discharge efficiency and discharge power. The linear fitting expression between the two variables is given as follows:

$$y = -6\times10^{-3} W_{\mathrm{e}} + 0.9718 \tag{14}$$

In the equation, W_{e} represents the discharge power of the battery.

As shown in Fig. 5, the proposed method, based on the dual-polarization equivalent circuit model and enhanced by the incorporation of a diode into the power battery model of new energy vehicles, effectively eliminates the theoretical errors caused by hysteresis effects. This enables accurate estimation of the battery's state of charge (*SOC*).

As a result, there is a high degree of consistency between the discharge efficiency estimated by the proposed method and that of the linear discharge mode.

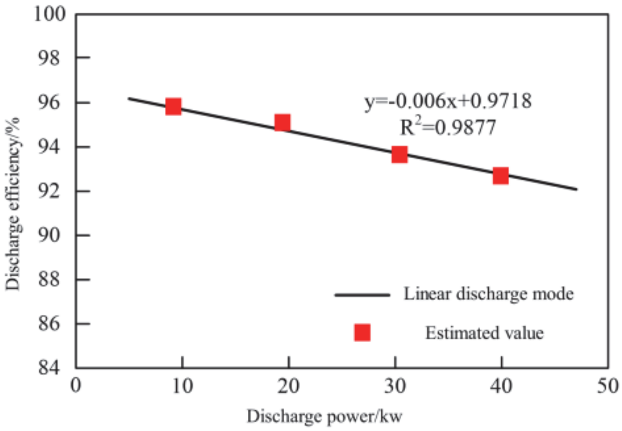

Figure 5 Discharge efficiency fitting diagram

Quantitative validation results show: The root mean square error (RMSE) of *SOC* estimation is 0.012, and the mean absolute error (MAE) is 0.008; the RMSE of voltage prediction is 0.15 V, and the MAE is 0.12 V (see Tab. 2). All experiments were repeated 3 times, and the 95% confidence interval of discharge efficiency results is [0.962, 0.988], confirming statistical robustness.

Table 2 Quantitative validation indicators

Validation Index	SOC Estimation	Voltage Prediction
RMSE	0.012	0.15 V
MAE	0.008	0.12 V
95% Confidence Interval (Discharge Efficiency)	-	[0.962, 0.988]

6 CONCLUSION

This study presented a novel simulation framework for analyzing variable-current discharge in lithium-ion batteries. By integrating a diode into the dual-polarization equivalent circuit, the model effectively mitigates voltage hysteresis effects that impair *SOC* estimation. Coupled with an SVM-based OCV estimator and the ampere-hour integration method, the framework achieved *SOC* estimation errors within ±1.5%, voltage RMSE below 0.18 V, and maximum energy prediction error of 3.2% across simulated driving conditions. Results show that discharge duration shortens significantly at lower initial SOC, and discharge efficiency decreases at higher speeds. Compared with conventional ECM approaches, the diode-enhanced model improves accuracy and robustness, providing a practical tool for intelligent battery management systems. Future work will extend validation to wide temperature ranges and incorporate experimental datasets to strengthen applicability.

7 REFERENCES

[1] He, H., Xiong, R., & Fan, J. (2012). State of charge estimation for lithium-ion batteries using an improved the venin model with temperature compensation. *Journal of Power Sources*, *208*, 163-171. https://doi.org/10.1016/j.jpowsour.2012.03.081

[2] Lai, X., Zheng, Y., & Sun, T. (2018). A comparative study of different equivalent circuit models for estimating state-of-charge of lithium-ion batteries. *Electrochimica Acta*, *259,* 566-577. https://doi.org/10.1016/j.electacta.2017.10.153

[3] Nejad, S., Gladwin, D. T., & Stone, D. A. (2016). A systematic review of lumped-parameter equivalent circuit models for real-time estimation of lithium-ion battery states. *Journal of Power Sources*, *316*, 183-196. https://doi.org/10.1016/j.jpowsour.2016.03.042

[4] Shen, W. X., Chan, C. C., Lo, E. W. C. et al. (2002). Estimationofbatteryavailablecapacityundervariabledischargecurrents. *Journal of Power Sources*, *103*(2), 180-187. https://doi.org/10.1016/s0378-7753(01)00840-0

[5] Fuller, M. E. (2014). A battery model for constant-power discharge including rate effects. *Energy Conversion and Management*, *88*, 199-205. https://doi.org/10.1016/j.enconman.2014.08.015

[6] Xu, T., Peng, Z., & Wu, L. (2021). A novel data-driven method for predicting the circulating capacity of lithium-ion battery under random variable current. *Energy*, *218*, 119530. https://doi.org/10.1016/j.energy.2020.119530

[7] Zarei-Jelyani, M., Loghavi, M. M., Babaiee, M. et al. (2023). The significance of charge and discharge current densities in the performance of vanadium redox flow battery. *Electrochimica Acta*, *443*, 141922. https://doi.org/10.1016/j.electacta.2023.141922

[8] Gong, M., Chen, J., Chen, J. et al. (2024). Discharge characteristic analysis of lithium-ion batteries for electric vehicles under multi-cycle conditions. *Journal of Power Sources*, *576*, 233210. https://doi.org/10.1016/j.jpowsour.2024.233210

[9] Cho, S., Jeong, H., Han, C. et al. (2012). State-of-charge estimation for lithium-ion batteries under various operating conditions using an equivalent circuit model. *Computers & Chemical Engineering*, *41*, 1-9. https://doi.org/10.1016/j.compchemeng.2012.02.003

[10] Liu, X., Li, W., & Zhou, A. (2018). PNGV equivalent circuit model and SOC estimation algorithm for lithium battery pack adopted in AGV vehicle. *IEEE Access*, *6*, 23639-23647. https://doi.org/10.1109/access.2018.2812421

[11] Yue, F., Zhang, G., Zhang, J. et al. (2017). Numerical simulation of transport characteristics of Li-ion battery in different discharging modes. *Applied Thermal Engineering*, *126*, 70-80. https://doi.org/10.1016/j.applthermaleng.2017.07.151

[12] Mei, W., Li, H., Zhao, C. et al. (2020). Numerical study on thermal characteristics comparison between charge and discharge process for lithium ion battery. *International Journal of Heatand Mass Transfer*, *162*, 120319. https://doi.org/10.1016/j.ijheatmasstransfer.2020.120319

[13] Chen, H., Zhang, T., Hua, Y. et al. (2023). Simulation study on the interaction between the battery module and bus bar under typical driving conditions of electric vehicles. *Case Studies in Thermal Engineering*, *45*, 103006. https://doi.org/10.1016/j.csite.2023.103006

[14] Nikdel, M. (2014). Various battery models for various simulation studies and applications. *Renewable and Sustainable Energy Reviews*, *32*, 477-485. https://doi.org/10.1016/j.rser.2014.01.048

[15] Pesaran, A. A. (2002). Battery thermal models for hybrid vehicle simulations. *Journal of Power Sources*, *110*(2), 377-382. https://doi.org/10.1016/s0378-7753(02)00200-8

[16] Tang, M. C., Cao, J., Gong, D. Q. et al. (2024). Simulation modelling of electric vehicle charging recommendations based on Q-learning. *International Journal of Simulation Modelling*, *23*(3), 495-506. https://doi.org/10.2507/IJSIMM23-3-CO11

[17] Reddy, B. V. K., Barry, M., Li, J. et al. (2012). A fluid-thermo-electric coupled field an alysis of a novel integrated thermo electric device. *Energy Procedia*, *14*, 2088-2095. https://doi.org/10.1016/j.egypro.2011.12.1212

[18] Hu, X., Li, S., & Peng, H. (2012). A comparative study of equivalent circuit models for Li-ion batteries. *Journal of Power Sources*, *198*, 359-367. https://doi.org/10.1016/j.jpowsour.2011.10.013

[19] Sitterly, M., Yin, G. G., & Wang, C. (2011). Enhanced

identification of battery models for real-time battery management. *IEEE Transactions on Sustainable Energy*, *2*(3), 300-308. https://doi.org/10.1109/tste.2011.2116813
[20] Du, H. & Chen, J. (2023). An improved antcolony algorithm for new energy industry resource allocation in cloud environment. *Technical Gazette*, *30*(1), 153-157. https://doi.org/10.17559/TV-20220712164019
[21] Laue, V., Röder, F., & Krewer, U. (2021). Practical identifiability of electrochemical P2D models for lithium-ion batteries. *Journal of Applied Electrochemistry*, *51*(9), 1253-1265. https://doi.org/10.1007/s10800-021-01579-5
[22] Meng, J., Ricco, M., Luo, G. et al. (2017). An overview and comparison of online implementable SOC estimation methods for lithium-ion battery. *IEEE Transactions on Industry Applications*, *54*(2), 1583-1591. https://doi.org/10.1109/TIA.2017.2775179
[23] Christophersen, J. P., Morrison, J., Morrison, W. et al. (2012). Rapid impedance spectrum measurements for state-of-health assessment of energy storage devices. *SAE International Journal of Passenger Cars - Electronic and Electrical Systems*, *5*(2012-01-0657), 246-256. https://doi.org/10.4271/2012-01-0657
[24] Savran, E., Karpat, E., & Karpat, F. (2024). GA and WOA-based optimization for electric power train efficiency. *International Journal of Simulation Modelling*, *23*(4), 599-610. https://doi.org/10.2507/IJSIMM23-4-699
[25] Wang, S. & Chen, Y. (2023). Effect of battery pack connection on vehicle ride comfort. *Technical Gazette*, *30*(2), 584-589. https://doi.org/10.17559/TV-20221109024651

Contact information:

Houcheng ZHAO, Associate Professor
1) Geely University of China,
Chengdu, Sichuan 641423, China
2) Ulaanbaatar Erdem University,
Mongolia School of Management,
999097, Ulaanbaatar, Mongolia
E-mail: zhaohoucheng163@163.com

Juan LI, Lecturer
Sichuan Hope Automobile Vocational College,
School of Automotive Engineering,
Ziyang, Sichuan 641399, China

Yaorong YANG, Associate Researcher
(Corresponding author)
Geely University of China,
Chengdu, Sichuan 641423, China
E-mail: 13659018562@163.com

Chun GAN, Lecturer
Sichuan Hope Automobile Vocational College,
School of Automotive Engineering,
Ziyang, Sichuan 641399, China

Yanxi OU, Lecturer
Geely University of China,
Chengdu, Sichuan 641423, China

B. OCHGEREL, Professor
Ulaanbaatar Erdem University,
Mongolia School of Management,
999097, Ulaanbaatar, Mongolia

Y. OYUNTUGALAG, Professor
Ulaanbaatar Erdem University,
Mongolia School of Management,
999097, Ulaanbaatar, Mongolia